Journal of Materials Chemistry A

PAPER

View Article Online
View Journal | View Issue

Cite this: J. Mater. Chem. A, 2019, 7, 19522

Structural engineering of pyrrolo[3,4-*f*]benzotriazole-5,7(2*H*,6*H*)-dione-based polymers for non-fullerene organic solar cells with an efficiency over 12%†

Birhan A. Abdulahi,[ab] Xiaoming Li,[c] Mariza Mone,[b] Bisrat Kiros,[a] Zewdneh Genene,[d] Shanlin Qiao,[c] Renqiang Yang,*[e] Ergang Wang*[b] and Wendimagegn Mammo*[a]

Received 14th June 2019
Accepted 25th July 2019

DOI: 10.1039/c9ta06385d

rsc.li/materials-a

In this work, we have synthesized two wide band gap donor polymers based on benzo[1,2-*b*:4,5-*b*′] dithiophene (BDT) and pyrrolo[3,4-*f*]benzotriazole-5,7(2*H*,6*H*)-dione (TzBI), namely, **PBDT-TzBI** and **PBDT-F-TzBI** and studied their photovoltaic properties by blending them with ITIC as an acceptor. Polymer solar cell devices made from **PBDT-TzBI**:ITIC and **PBDT-F-TzBI**:ITIC exhibited power conversion efficiencies (PCEs) of 9.22% and 11.02% and while annealing at 160 °C, improved the device performances to 10.24% and 11.98%, respectively. Upon solvent annealing with diphenyl ether (DPE) (0.5%) and chlorobenzene (CB), the PCE of the **PBDT-F-TzBI**-based device increased to 12.12%. The introduction of the fluorinated benzodithiophene (BDT-F) moiety on the backbone of **PBDT-F-TzBI** improved the open circuit voltage, short circuit current and fill factor simultaneously. The high PCEs of the **PBDT-F-TzBI**:ITIC-based devices were supported by comparison and analysis of the optical and electronic properties, the charge carrier mobilities, exciton dissociation probabilities, and charge recombination behaviors of the devices.

Introduction

Organic solar cells (OSCs) attracted the attention of the scientific community due to the possibility of manufacturing light weight, flexible, and easily printed next generation solar cell devices using the roll-to-roll printing technique.[1–6] Although PCBM derivatives were the acceptors of choice in the past, recent years have witnessed the rapid development of non-fullerene acceptors because of the flexibility of choosing different donor materials for tunable optical and energetic properties of the active layer of OSCs.[1,7–15] In the last five years, non-fullerene OSCs showed impressively high PCEs exceeding 15% using fused-ring structured electron acceptors.[11,16] These results motivate researchers to design new donor polymers with desirable properties, such as broad and intense absorption to enhance short-circuit current (J_{sc}) and suitable energy levels to improve open-circuit voltage (V_{oc}). The donor–acceptor (D–A) alternating conjugated polymer synthesis is the commonly used strategy to prepare efficient donor polymers. In this regard, among the commonly investigated wide band-gap polymers are thieno[3,4-*c*]pyrrole-4,6-dione[17–19] (TPD)-, [2,1,3]benzothiadiazole[20–27] (BT)- and 2*H*-benzo[*d*][1,2,3]triazole[8,28–31] (BTz)-based D–A conjugated polymers. Yin *et al.*[32] combined TPD and BT to garner the advantages of solubility and deep HOMO energy levels simultaneously, and synthesized the [2,1,3]benzothiadiazole-5,6-dicarboxylic imide-based acceptor monomer 4,8-bis(5-bromothiophen-2-yl)-6-(2-ethylhexyl)-5*H*-[1,2,5]thiadiazolo[3,4-*f*]isoindole-5,7(6*H*)-dione. By copolymerizing this compound with (4,8-bis(5-(2-butyloctyl)thiophen-2-yl)benzo[1,2-*b*:4,5-*b*′] dithiophene-2,6-diyl)bis(trimethylstannane), a polymer was obtained which was blended with $PC_{71}BM$ to fabricate solar cells that afforded a PCE of 5.19% with V_{oc} of 0.91 V, J_{sc} of 11.59 mA cm^{-2} and FF of 0.49. Later on McCulloch *et al.*[33] synthesized other [2,1,3]benzothiadiazole-5,6-dicarboxylic imide-based polymers and reported a high PCE of 8.3% with a V_{oc} of 0.80 V, J_{sc} of 16.45 mA cm^{-2} and FF of 0.63.

Cao *et al.*[34] modified the [2,1,3]benzothiadiazole-5,6-dicarboxylic imide moiety by replacing the BT unit with BTz to prepare the acceptor monomer 4,8-bis(5-bromothiophen-2-

[a]Department of Chemistry, Addis Ababa University, P.O. Box 33658, Addis Ababa, Ethiopia. E-mail: wendimagegn.mammo@aau.edu.et
[b]Department of Chemistry and Chemical Engineering, Chalmers University of Technology, SE-412 96 Göteborg, Sweden. E-mail: ergang@chalmers.se
[c]College of Chemistry and Pharmaceutical Engineering, Hebei University of Science and Technology, Shijiazhuang 050018, P. R. China
[d]Department of Chemistry, Ambo University, P.O. Box 19, Ambo, Ethiopia
[e]CAS Key Laboratory of Bio-based Materials, Qingdao Institute of Bioenergy and Bioprocess Technology, Chinese Academy of Sciences, Qingdao 266101, China. E-mail: yangrq@qibebt.ac.cn

† Electronic supplementary information (ESI) available. See DOI: 10.1039/c9ta06385d

yl)-2,6-dioctyl-[1,2,3]triazolo[4,5-*f*]isoindole-5,7(2*H*,6*H*)-dione (Br_2-TzBI), which was envisaged to impart lower energy levels on the resulting D–A polymers with improved solubility. By copolymerizing Br_2-TzBI with the weak electron donor monomer, (4,8-bis(5-(2-ethylhexyl)thiophen-2-yl)benzo[1,2-*b*:4,5-*b*′] dithiophene-2,6-diyl)bis(trimethylstannane) (Sn_2-BDT), **PTzBIBDT** was obtained, which afforded a high PCE of 8.63% with a V_{oc} of 0.87 V, J_{sc} of 13.50 mA cm^{-2} and FF of 0.74 in solar cell devices with $PC_{71}BM$ as an acceptor.[34] Furthermore, by blending **PTzBIBDT** with ITIC, the J_{sc} was enhanced to 18.29 mA cm^{-2} and a high PCE of 10.24% with a V_{oc} of 0.87 V and FF of 0.64 was demonstrated.[35] Cao *et al.*[36] further replaced the 5-(2-ethylhexyl) thiophene units attached to the BDT moiety of **PTzBIBDT** with 4-(2-ethylhexyl)phenyl units and synthesized PTzBI-Ph. The solar cells fabricated from the blend of PTzBI-Ph with ITIC gave improved V_{oc} and FF values of 0.92 V and 0.68, respectively. However, the J_{sc} of the device dropped to 16.39 mA cm^{-2} to give a PCE of 10.19%.[36] In addition, Cao *et al.*[37] prepared different kinds of TzBI-based polymers by incorporating alkyl side groups and studied their photovoltaic performances with ITIC as an acceptor and registered a decent PCE of 7.28%. When the acceptor was changed to IT-2F, the performances of these devices were improved and a certified PCE of 12.25% with enhanced J_{sc} and FF could be achieved (ESI, Table S1†). These results show that enhancing V_{oc}, J_{sc} and FF simultaneously is still challenging for solar cells fabricated from TzBI-based polymer donors using ITIC as an acceptor. Clearly, there is room for further improvement in the performances of solar cells made of TzBI-based polymers with some structural modifications. It is known that introduction of fluorine atoms in the polymer structure makes the HOMO and LUMO energy levels of the polymer deeper, thereby enhancing V_{oc}.[38] It has also been shown that enhanced inter/intramolecular interactions of the polymer can improve crystallinity and facilitate charge transport which results in improved J_{sc} and FF values.[38–41] Taking these advantages into consideration, we decided to use a fluorine-containing BDT-based monomer **3** (Scheme 1) as an electron donor and polymerized it with TzBI-based monomer **1** to prepare **PBDT-F-TzBI** which was expected to enhance V_{oc}, J_{sc} and FF simultaneously, in non-fullerene OSCs. Thus, solar cells fabricated from the **PBDT-F-TzBI**:ITIC blend afforded a high PCE of 12.12% with a V_{oc} of 0.93 V, J_{sc} of 18.10 mA cm^{-2} and FF of 0.72, which is higher than those of the corresponding non-fluorinated **PBDT-TzBI**:ITIC-based solar cell devices. To investigate the reasons behind the variations in performances of the solar cells, we have studied the optical and electronic properties, the morphology, charge carrier mobility, exciton dissociation and charge recombination behaviors of the corresponding devices.

Results and discussion

Synthesis of monomers and polymers

The chemical structures of the polymers are shown in Scheme 1. The TzBI-based acceptor monomer, 4,8-bis(5-bromothiophen-2-yl)-2-(2-ethylhexyl)-6-octyl-[1,2,3]triazolo[4,5-*f*]isoindole-5,7(2*H*,6*H*)-

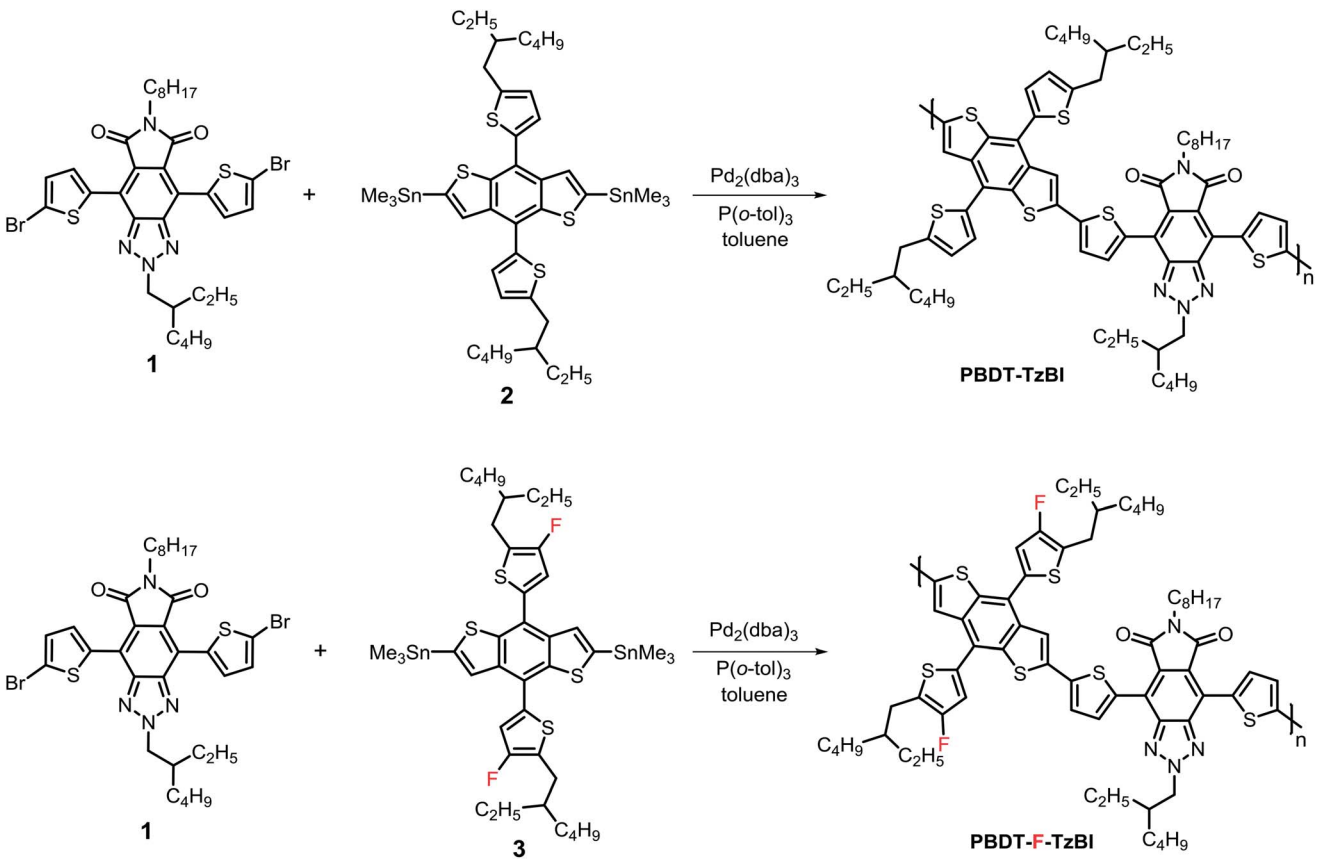

Scheme 1 Synthesis of PBDT-TzBI and PBDT-F-TzBI.

dione (**1**) was synthesized by modifying procedures reported in the literature (Scheme S1, ESI†).[34] In this work, we have introduced a branched side chain on the benzotriazole unit of **1** to enhance the solubility of the polymer. Compound **1** was copolymerized with the BDT-based monomers (4,8-bis(5-(2-ethylhexyl)thiophen-2-yl)benzo[1,2-*b*:4,5-*b*′]dithiophene-2,6-diyl)bis(trimethylstannane) (**2**) and (4,8-bis(5-(2-ethylhexyl)-4-fluorothiophen-2-yl)benzo[1,2-*b*:4,5-*b*′]dithiophene-2,6-diyl)bis(trimethylstannane) (**3**) at 110 °C in toluene by means of the Stille coupling polymerization reaction, to yield poly-4-(5-(4,8-bis(5-(2-ethylhexyl)thiophen-2-yl)-6-methylbenzo[1,2-*b*:4,5-*b*′]dithiophen-2-yl)thiophen-2-yl)-2-(2-ethylhexyl)-8-(5-methylthiophen-2-yl)-6-octyl-[1,2,3]triazolo[4,5-*f*]isoindole-5,7(2*H*,6*H*)dione (**PBDT-TzBI**) and poly-4-(5-(4,8-bis(5-(2-ethylhexyl)-4-fluorothiophen-2-yl)-6-methylbenzo[1,2-*b*:4,5-*b*′]dithiophen-2-yl)thiophen-2-yl)-2-(2-ethylhexyl)-8-(5-methylthiophen-2-yl)-6-octyl-[1,2,3]triazolo[4,5-*f*]isoindole-5,7(2*H*,6*H*)-dione (**PBDT-F-TzBI**), respectively. The polymers were Soxhlet-extracted with methanol and diethyl ether to remove low molecular weight oligomers, and then with chloroform. The chloroform extracts were precipitated from methanol, filtered and dried to afford **PBDT-TzBI** and **PBDT-F-TzBI**. Both polymers were soluble in chloroform, chlorobenzene, and *o*-dichlorobenzene. The molecular weights of the polymers were determined by gel permeation chromatography (GPC) at 150 °C, using 1,2,4-trichlorobenzene as the eluent. The M_n of **PBDT-TzBI** and **PBDT-F-TzBI** were found to be 26.9 and 16.5 kDa, with polydispersity indices of 3.8 and 4.1, respectively.

Thermal properties

The thermal stabilities of the polymers were evaluated by thermogravimetric analysis (TGA), as shown in Fig. S1, ESI.† The decomposition temperature (T_d) of **PBDT-F-TzBI** was above 430 °C, revealing good enough thermal stability for photovoltaic applications.

Optical and electrochemical properties of PBDT-TzBI and PBDT-F-TzBI

The UV-Vis absorption spectra of the polymers were recorded in $CHCl_3$ solution and as thin films coated on glass slides, and are shown in Fig. 1. Both **PBDT-TzBI** and **PBDT-F-TzBI** showed broad absorptions in the range between 350 and 700 nm. The thin film absorption of **PBDT-TzBI** was red-shifted compared to that in $CHCl_3$ solution. This revealed that the **PBDT-TzBI** had a strong π–π stacking property in the solid state. On the other hand, the bathochromic shift in the solid-state absorption spectrum of **PBDT-F-TzBI** was much less pronounced than that in solution, indicating the strong aggregation of **PBDT-F-TzBI** in solution, which can be caused by stronger intermolecular interactions caused by the introduction of fluorine atoms in the polymer backbone. The onsets of absorption of thin-films of **PBDT-TzBI** and **PBDT-F-TzBI** were found to be 687 and 684 nm, respectively. Accordingly, the optical band gaps were calculated from these to be 1.80 and 1.81 eV for **PBDT-TzBI** and **PBDT-F-TzBI**, respectively. This showed that the presence of fluorine had very little effect on the optical band gap of the polymer,

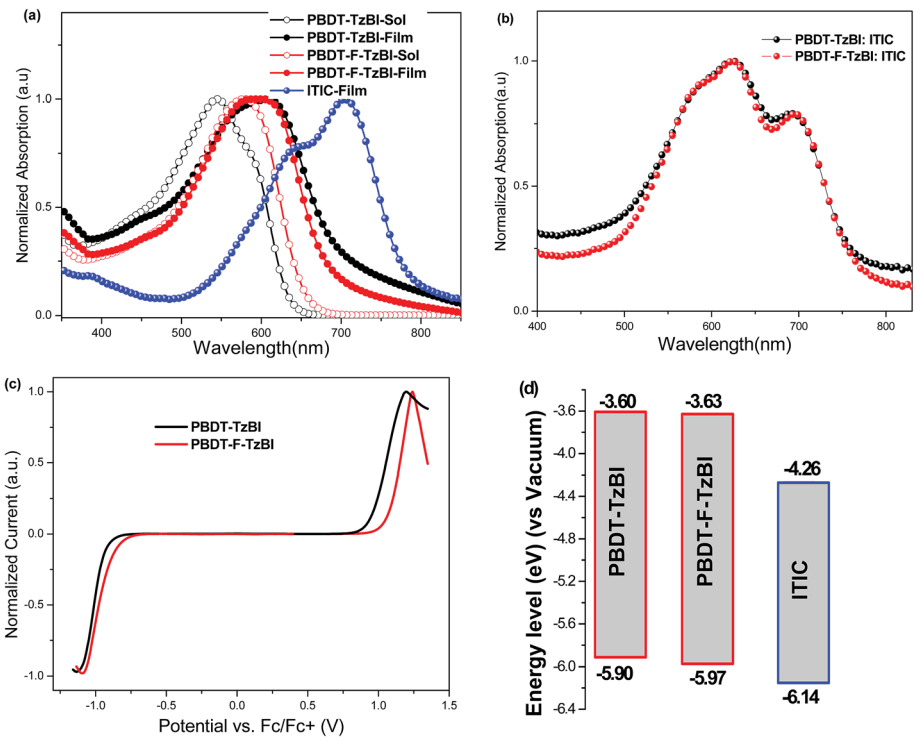

Fig. 1 (a) Normalized UV-Vis absorption spectra of PBDT-TzBI, PBDT-F-TzBI, and ITIC in solutions; (b) normalized UV-Vis absorption spectra of the blends of PBDT-TzBI:ITIC and PBDT-F-TzBI:ITIC in the solid state; (c) square wave voltammograms of PBDT-TzBI and PBDT-F-TzBI; (d) energy level diagram of the polymers and ITIC based on cyclic voltammetry measurements.

Table 1 Optical and electrochemical properties of the copolymers

	Optical properties					Electrochemical properties	
	λ_{max}/nm						
Polymer	Sol	Film	λ_{onset}/nm	E_g^{opt}/eV	$E_{oxd.}$/V	HOMO/eV	LUMO/eV
PBDT-TzBI	545	608	687	1.80	0.77	−5.90	−3.60
PBDT-F-TzBI	578	598	684	1.81	0.84	−5.97	−3.63

since incorporating F atoms might have resulted in simultaneous lowering of the LUMO and HOMO energy levels of **PBDT-F-TzBI**.[9] The thin film absorptions of **PBDT-TzBI** and **PBDT-F-TzBI** were complementary to that of ITIC in the wavelength region from 400 nm to 800 nm (Fig. 1b). Thus, high J_{sc}s could be generated from solar cell devices fabricated from blends of the polymers with ITIC. Temperature-dependent absorbance measurements were done to study the aggregation properties of **PBDT-F-TzBI** and **PBDT-TzBI** in *o*-DCB solution (Fig. S2, ESI†). When the solutions were warmed up from 10 to 90 °C, the absorptions of the polymers were blue-shifted and the absorption maxima were decreased. This proved that the polymers exhibited strong interchain interactions in *o*-DCB at low temperature.[42–44]

Square wave voltammetry was used to estimate the frontier molecular orbital energy levels of the polymers. The HOMO and LUMO levels were estimated from the oxidation and reduction peak potentials of the polymers, relative to the ferrocene/ferrocenium (Fc/Fc^+) redox couple, using the formula HOMO $= -(E_{ox} + 5.13)$ eV and LUMO $= -(E_{red} + 5.13)$ eV, where E_{ox} and E_{red} are the oxidation and reduction peak potentials, respectively. Thus, the HOMO energy levels were determined to be −5.90 and −5.97 eV, for **PBDT-TzBI** and **PBDT-F-TzBI**, respectively (Fig. 1, Table 1) while the LUMO levels were found to be −3.60 and −3.63 eVs for **PBDT-TzBI** and **PBDT-F-TzBI**, respectively. The HOMO energy levels determined from cyclic voltammetry (CV) measurements (Fig. S3, ESI†) showed similar trends to those obtained from SWV measurements. Under similar conditions, the HOMO and LUMO energy levels of ITIC were determined to be −6.14 and −4.26 eVs (Fig. S3, ESI†). The deeper HOMO energy level of **PBDT-F-TzBI** is attributed to the inductive electron withdrawing effects of the fluorine atoms from the donor moiety on the polymer backbone.

Photovoltaic properties

The photovoltaic performances of **PBDT-TzBI** and **PBDT-F-TzBI** were investigated using ITIC as an acceptor with the device geometry ITO/PEDOT:PSS/polymer:ITIC (1:1)/PDINO/Al (PDINO = perylene diimide functionalized with amino *N*-oxide which is used as an electron transport layer) and were characterized under AM 1.5G illumination at 100 mW cm^{-2} with a solar simulator. The photovoltaic parameters of the polymers are summarized in Table 2. Fig. 2 shows *J*–*V* curves and the external quantum efficiency (EQE) spectra of **PBDT-TzBI**:ITIC- and **PBDT-F-TzBI**:ITIC-based solar cell devices.

The OSC devices made from **PBDT-TzBI**:ITIC exhibited a PCE of 9.22% with a V_{oc} of 0.88 V, J_{sc} of 16.37 mA cm^{-2} and FF of 0.64, while the device based on **PBDT-F-TzBI**:ITIC scored a PCE of 11.02% with a V_{oc} of 0.97 V, J_{sc} of 16.72 mA cm^{-2} and FF of 0.68. **PBDT-F-TzBI**-based devices exhibited higher V_{oc} compared with **PBDT-TzBI**-based devices as a result of the presence of fluorine atoms that make the HOMO levels of the polymer deeper. Thermal annealing of BHJ solar cells is known to support the formation of favorable morphology by tuning the domain sizes and aggregation properties of certain donor and acceptor materials.[6,45] Hence, to improve the J_{sc} and FF of our PSCs, the devices were thermally annealed at 160 °C for 10 min. The PCEs of the devices made from blends of **PBDT-TzBI**:ITIC and **PBDT-F-TzBI**:ITIC were both improved to 10.24% and 11.98%, respectively, due to simultaneous improvements in both J_{sc} and FF as shown in Table 2. It is known that efficient exciton dissociation and charge transfer requires bicontinuous interpenetrating networks between electron donors and acceptors in the BHJ active layer of the solar cell.[9] Solvent additives facilitate molecular reorganization of the donor and acceptor materials and lead to the development of different crystalline structures in the active layers. This promotes the formation of the desired morphology for efficient exciton dissociation and charge transport in the BHJ.[35,46] Favorable morphology is a characteristic nature of PSCs to facilitate charge transport properties that enhance the performance by improving J_{sc} and FF. Thus, when diphenyl ether (DPE) (0.5%) was used as an additive and CB solvent vapor annealing was conducted, the PCE of the **PBDT-F-TzBI**-based device increased to 12.12% with a V_{oc} of 0.93 V, J_{sc} of 18.10 mA cm^{-2} and FF of 0.72. The slightly improved J_{sc} and FF of the device may be due to the favorable molecular orientation caused by the processing additive. The high PCE of the **PBDT-F-TzBI**:ITIC-based solar cell device makes

Table 2 Photovoltaic parameters of devices measured under AM 1.5G, 100 mW cm^{-2}

Donor:acceptor	V_{oc} [V]	J_{sc} [mA cm^{-2}]	FF	PCE [%]
PBDT-TzBI-:ITIC	0.88	16.37	0.64	9.22
PBDT-F-TzBI:ITIC	0.97	16.72	0.68	11.02
PBDT-TzBI-:ITIC[a]	0.84	17.78(17.16)[c]	0.69	10.24
PBDT-F-TzBI:ITIC[a]	0.97	18.00	0.70	11.98
PBDT-F-TzBI:ITIC[b]	0.93	18.10(17.47)[c]	0.72	12.12

[a] The devices were thermally annealed at 160 °C for 10 min. [b] 0.5% DPE additive and CB vapor annealing was used. [c] Photocurrents obtained by integrating the EQE with the AM 1.5G spectrum are given in the parentheses.

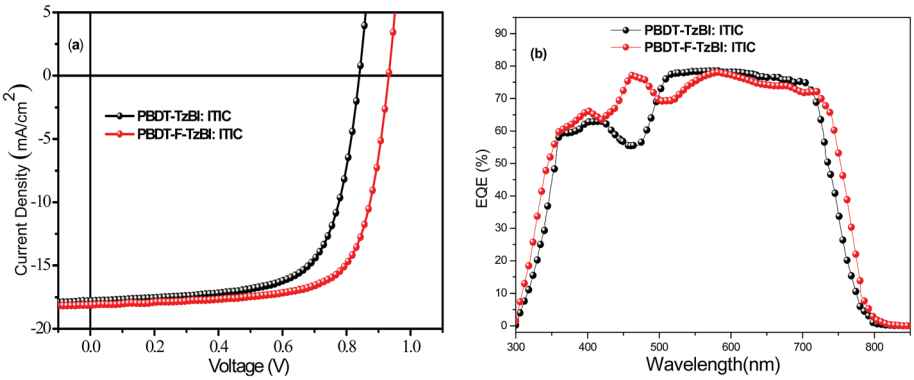

Fig. 2 (a) Current density–voltage characteristics, (b) EQE curves, of **PBDT-TzBI**:ITIC- and **PBDT-F-TzBI**:ITIC-based solar cells.

PBDT-F-TzBI as one of the promising candidates for practical application in OSCs.

To evaluate the spectral responses of the PSCs and the accuracies of the photocurrents from the *J*–*V* measurements, external quantum efficiency (EQE) measurements were carried out (Fig. 2). Both **PBDT-TzBI**:ITIC- and **PBDT-F-TzBI**:ITIC-based solar cells showed maximum photoresponses with EQEs of more than 75% in the range between 500 and 700 nm. The photoresponses over the region between 300 and 800 nm in the EQE curves are consistent with the absorption profiles of the blend films suggesting that both the donor and acceptor materials contributed to the photocurrents. The photocurrents calculated by integrating the EQE spectra with AM 1.5G solar spectrum are consistent with the J_{sc} values obtained from the *J*–*V* measurements, with less than 5% difference.

Film morphology

Atomic force microscopy (AFM) and transmission electron microscopy (TEM) measurements were employed to study the surface roughness and phase separation of the blend films, and the images are shown in Fig. 3. The **PBDT-F-TzBI**:ITIC and **PBDT-TzBI**:ITIC blend films showed smooth surfaces with root mean-square (RMS) roughnesses of 0.97 and 1.07 nm, respectively. The presence of fluorine in **PBDT-F-TzBI** exerted limited effect on the morphology of the blend as indicated by AFM. The TEM images of the blends presented very fine features, indicating good miscibility with nanometer-scale microphase separation between the donor and the acceptor materials, which is favorable for charge separation and transport.[35] The AFM and TEM images of the blends revealed that the film morphologies of both blend films were optimal but cannot tell

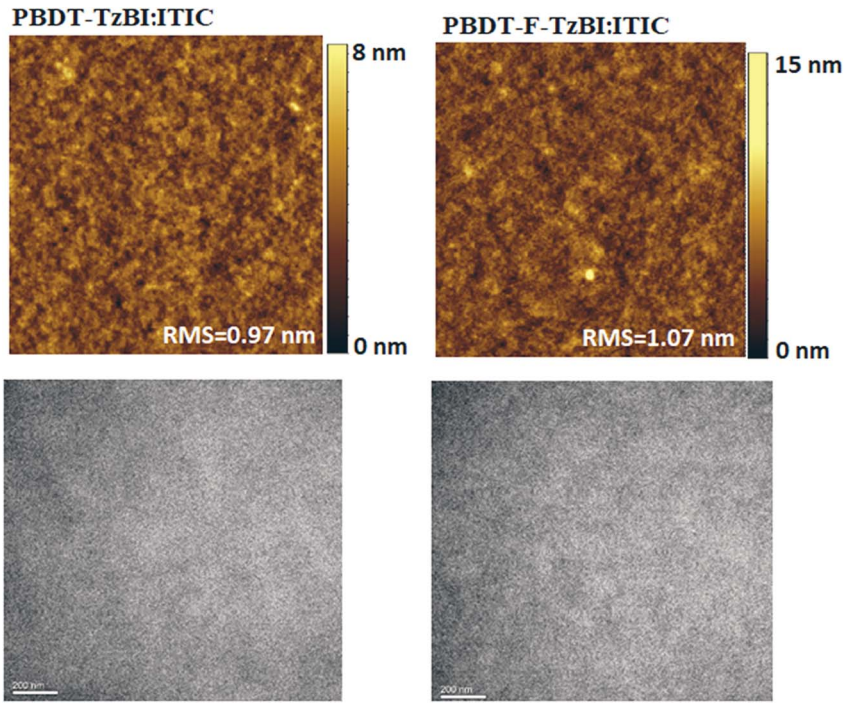

Fig. 3 AFM topography (5 × 5 nm) and TEM images of the optimized **PBDT-F-TzBI**:ITIC and **PBDT-TzBI**:ITIC blend films.

Table 3 SCLC hole and electron mobilities of the blend films

Donor:acceptor	SCLC μ_h ($cm^2\ V^{-1}\ s^{-1}$)	SCLC μ_e ($cm^2\ V^{-1}\ s^{-1}$)	μ_h/μ_e
PBDT-TzBI:ITIC	1.1×10^{-4}	1.6×10^{-4}	0.69
PBDT-F-TzBI:ITIC	2.0×10^{-4}	2.3×10^{-4}	0.87

the reason for the higher J_{sc} and FF of **PBDT-F-TzBI**:ITIC-based devices.

Charge carrier mobility

To characterize the charge transport properties of the polymer:ITIC blends, the electron (μ_e) and hole (μ_h) mobilities of the PSCs were measured by the space charge limited current (SCLC) method using electron-only devices with the configuration ITO/ZnO/active layer/PIDNO/Al and hole-only devices with the configuration ITO/PEDOT:PSS/active layer/Au, respectively. The corresponding hole and electron mobilities are summarized in Table 3. The **PBDT-TzBI**:ITIC and **PBDT-F-TzBI**:ITIC blend films exhibited decent μ_h and μ_e in the order of 10^{-4} $cm^2\ V^{-1}\ s^{-1}$, which were comparable with those of other TzBI-based polymers.[36] Relatively higher and balanced μ_h and μ_e were found for the **PBDT-F-TzBI**:ITIC blend than for the **PBDT-TzBI**:ITIC blend. It is known that balanced hole and electron mobilities can reduce bimolecular recombination to give high photocurrent and FF, which supports the higher J_{sc} and FF of **PBDT-F-TzBI**:ITIC-based solar cells.[10,44,47,48]

Exciton dissociation and charge recombination behavior

To study the exciton dissociation probability in **PBDT-TzBI**- and **PBDT-F-TzBI**-based devices, the photocurrent density (J_{ph}) was evaluated as a function of the effective voltage (V_{eff}) as shown in Fig. 4. J_{ph} is the difference between illuminated and dark current, and V_{eff} is the difference between V_{oc} and V_a, where V_{oc} is the voltage at zero J_{ph} and V_a is the applied voltage. The exciton dissociation probability of a device can be calculated as $P_{diss} = J_{ph}/J_{sat}$, where J_{sat} stands for saturation photocurrent density.[49–51] Under short circuit conditions, the P_{diss}s of **PBDT-TzBI**:ITIC- and **PBDT-F-TzBI**:ITIC-based devices were calculated to be 95.8% and 97.4%, respectively. The relatively higher P_{diss} of the **PBDT-F-TzBI**-based device showed better exciton dissociation and charge collection than its **PBDT-TzBI**-based counterpart, which partly contributed to the higher J_{sc} and FF of the **PBDT-F-TzBI**-based devices.[12,51,52]

To investigate the charge recombination behaviors of the devices, we studied the effect of light intensity (P_{light}) on the short-circuit current density (J_{sc}) of the PSCs (Fig. 4). P_{light} and J_{sc} are related to each other according to the power law as $J_{sc} \propto P^S$. The value of S should be 1 when all free carriers are swept out and collected at the electrodes prior to recombination, whereas when the value of S is less than 1, the presence of some degree of bimolecular recombination is anticipated.[53–55] The S value of **PBDT-F-TzBI**:ITIC is 0.98, which is closer to 1, and indicates the presence of weak bimolecular recombination and efficient carrier transportation compared to **PBDT-TzBI**:ITIC ($S = 0.97$). This reduced bimolecular recombination correlates with the higher and balanced charge carrier mobility of the corresponding device that contributed partly to its higher J_{sc} and FF.[54] We have thus demonstrated relatively higher and more balanced carrier mobility, better exciton dissociation and weaker bimolecular recombination for **PBDT-F-TzBI**-based devices justifying the higher J_{sc} and FF that resulted in a higher PCE (>12%) compared to their non-fluorinated analogs.

In conclusion, two wide band gap donor polymers, **PBDT-TzBI** and **PBDT-F-TzBI**, were successfully synthesized by polymerization of TzBI-based monomer **1** with BDT-based monomers (4,8-bis(5-(2-ethylhexyl)thiophen-2-yl)benzo[1,2-*b*:4,5-*b*′]dithiophene-2,6-diyl)bis(trimethylstannane) (**2**) and (4,8-bis(5-(2-ethylhexyl)-4-fluorothiophen-2-yl)benzo[1,2-*b*:4,5-*b*′]dithiophene-2,6-diyl)bis(trimethylstannane) (**3**), respectively. The PSCs fabricated from blends of **PBDT-TzBI** and **PBDT-F-TzBI** with ITIC annealed at 160 °C showed high PCEs of 10.24% and 11.98%, respectively. The presence of fluorine atom on the backbone of **PBDT-F-TzBI** lowered its HOMO energy level and improved its V_{oc} compared to **PBDT-TzBI**-based devices. Moreover, due to the presence of fluorine, higher charge carrier mobility, exciton dissociation probability and weak bimolecular recombination were observed for the **PBDT-F-TzBI**-based device. These properties explained the higher J_{sc} and FF of the **PBDT-F-TzBI**-based device that enhanced its overall performance compared to its **PBDT-TzBI**-based counterpart. Using

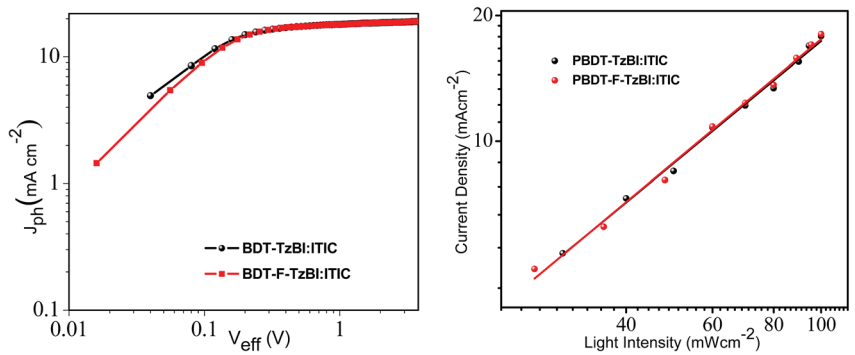

Fig. 4 (a) J_{ph}–V_{eff} characteristics and (b) dependence of J_{sc} on the light intensity of PBDT-TzBI- and PBDT-F-TzBI-based devices.

DPE (0.5%) as a processing additive and vapor phase annealing with CB, the PCE of the **PBDT-F-TzBI**-based device improved to 12.12% with a V_{oc} of 0.93 V, J_{sc} of 18.10 mA cm^{-2} and FF of 0.72, which is the highest value reported so far for TzBI-based polymers using ITIC as an acceptor. The results showed that **PBDT-F-TzBI** is among the most promising candidates for application in OSCs.

Experimental section

Materials characterization

The intermediate compounds and monomers were characterized by ^{1}H NMR (400 MHz) and ^{13}C NMR (100 MHz) using a Bruker Avance 400 NMR spectrometer. The molecular weights of the polymers were determined by size exclusion chromatography (SEC) on a Waters Alliance GPCV2000 with a refractive index detector using 1,2,4-trichlorobenzene as the eluent at 150 °C with a polystyrene standard calibration. Thermogravimetric analysis (TGA) was carried out on a METTLER TOLEDO thermogravimetric analyzer TGA/DSC 3+, from 50 to 550 °C at a heating rate of 10 °C min^{-1} under N_2 flow. A Perkin Elmer Lambda 900 UV-Vis-NIR spectrometer was used to measure the absorptions of the polymers. Square wave voltammetry (SWV) measurements were done on a CH-Instruments 650A electrochemical workstation using a three-electrode system. Platinum wires were used for both working and counter electrodes while Ag/Ag$^+$ was used as the reference electrode calibrated with the ferrocene/ferrocenium couple (Fc/Fc$^+$). The supporting electrolyte was tetrabutylammoniumhexafluorophosphate (Bu_4NPF_6) solution (0.1 M) in anhydrous acetonitrile.

PSC fabrication and characterization

Device fabrication and evaluations. Photovoltaic devices were fabricated with a conventional device structure of ITO/PEDOT:PSS/polymer:ITIC/PDINO/Al. The patterned ITO glass (sheet resistance = 15 Ω per square) was pre-cleaned in an ultrasonic bath with ITO detergent, deionized water, acetone, and isopropyl alcohol and treated in an ultraviolet-ozone chamber (PREEN II-862) for 13 min, then exposed to oxygen plasma for 3 min, twice. A thin layer (about 30 nm) of PEDOT:PSS was then spin-coated onto the ITO glass at 4000 rpm and baked at 150 °C for 15 min. Solutions of polymer/ITIC in CB were stirred overnight and spin-coated on top of the PEDOT:PSS layer to form the active layer of about 110–150 nm. The thickness of the active layer was measured using a Veeco Dektak 150 profilometer. PIDNO solution (in CH_3OH) was then spin-coated as an electron transfer layer. Finally, an Al (100 nm) metal electrode was thermally evaporated at about 4×10^{-4} Pa and the device area of 0.1 cm^2 was defined by a shadow mask. The current density–voltage (J–V) characteristics were recorded with a Keithley 2400 source measurement unit under simulated 100 mW cm^{-2} irradiation from a Newport solar simulator. The external quantum efficiencies (EQEs) were analyzed using a certified Newport incident photon conversion efficiency (IPCE) measurement system.

Conflicts of interest

There are no conflicts to declare.

Acknowledgements

W. Mammo, B. A. Abdulahi, B. K. and Z. G. acknowledge financial support from the International Science Programme (ISP), Uppsala University, Sweden. E. Wang thanks the Swedish Research Council, the Swedish Research Council Formas and The Knut and Alice Wallenberg Foundation (2017.0186, 2016.0059) for financial support. R. Yang thanks the National Natural Science Foundation of China (51773220, 21728401) for financial support.

References

1 G. Zhang, J. Zhao, P. C. Y. Chow, K. Jiang, J. Zhang, Z. Zhu, J. Zhang, F. Huang and H. Yan, Nonfullerene Acceptor Molecules for Bulk Heterojunction Organic Solar Cells, *Chem. Rev.*, 2018, **118**(7), 3447.
2 M. C. Scharber and N. S. Sariciftci, Efficiency of bulk-heterojunction organic solar cells, *Prog. Polym. Sci.*, 2013, **38**(12), 1929.
3 Z. C. Hu, L. Ying, F. Huang and Y. Cao, Towards a bright future: polymer solar cells with power conversion efficiencies over 10%, *Sci. China: Chem.*, 2017, **60**(5), 571.
4 K. A. Mazzio and C. K. Luscombe, The future of organic photovoltaics, *Chem. Soc. Rev.*, 2015, **44**(1), 78.
5 W. Cao and J. Xue, Recent progress in organic photovoltaics: device architecture and optical design, *Energy Environ. Sci.*, 2014, **7**(7), 2123.
6 L. Lu, T. Zheng, Q. Wu, A. M. Schneider, D. Zhao and L. Yu, Recent Advances in Bulk Heterojunction Polymer Solar Cells, *Chem. Rev.*, 2015, **115**(23), 12666.
7 C. B. Nielsen, S. Holliday, H.-Y. Chen, S. J. Cryer and I. McCulloch, Non-Fullerene Electron Acceptors for Use in Organic Solar Cells, *Acc. Chem. Res.*, 2015, **48**(11), 2803.
8 D. He, F. Zhao, J. Xin, J. J. Rech, Z. Wei, W. Ma, W. You, B. Li, L. Jiang, Y. Li and C. Wang, A Fused Ring Electron Acceptor with Decacyclic Core Enables over 13.5% Efficiency for Organic Solar Cells, *Adv. Energy Mater.*, 2018, **8**(30), 1802050.
9 A. Tang, B. Xiao, F. Chen, J. Zhang, Z. Wei and E. Zhou, The Introduction of Fluorine and Sulfur Atoms into Benzotriazole-Based p-Type Polymers to Match with a Benzotriazole-Containing n-Type Small Molecule: "The Same-Acceptor-Strategy" to Realize High Open-Circuit Voltage, *Adv. Energy Mater.*, 2018, **8**(25), 1801582.
10 Z. Li, X. Xu, W. Zhang, X. Meng, W. Ma, A. Yartsev, O. Inganäs, M. R. Andersson, R. A. J. Janssen and E. Wang, High Performance All-Polymer Solar Cells by Synergistic Effects of Fine-Tuned Crystallinity and Solvent Annealing, *J. Am. Chem. Soc.*, 2016, **138**(34), 10935.
11 J. Yuan, Y. Zhang, L. Zhou, G. Zhang, H.-L. Yip, T.-K. Lau, X. Lu, C. Zhu, H. Peng, P. A. Johnson, M. Leclerc, Y. Cao, J. Ulanski, Y. Li and Y. Zou, Single-Junction Organic Solar

Cell with over 15% Efficiency Using Fused-Ring Acceptor with Electron-Deficient Core, *Joule*, 2019, **3**(4), 1140.

12 Y. Wang, Y. Zhang, N. Qiu, H. Feng, H. Gao, B. Kan, Y. Ma, C. Li, X. Wan and Y. Chen, A Halogenation Strategy for over 12% Efficiency Nonfullerene Organic Solar Cells, *Adv. Energy Mater.*, 2018, **8**(15), 1702870.

13 W. Zhao, S. Li, H. Yao, S. Zhang, Y. Zhang, B. Yang and J. Hou, Molecular Optimization Enables over 13% Efficiency in Organic Solar Cells, *J. Am. Chem. Soc.*, 2017, **139**(21), 7148.

14 H. Zhang, H. Yao, J. Hou, J. Zhu, J. Zhang, W. Li, R. Yu, B. Gao, S. Zhang and J. Hou, Over 14% Efficiency in Organic Solar Cells Enabled by Chlorinated Nonfullerene Small-Molecule Acceptors, *Adv. Mater.*, 2018, **30**(28), 1800613.

15 Z. Luo, G. Li, W. Gao, K. Wu, Z.-G. Zhang, B. Qiu, H. Bin, L. Xue, F. Liu, Y. Li and C. Yang, A universal nonfullerene electron acceptor matching with different band-gap polymer donors for high-performance polymer solar cells, *J. Mater. Chem.A*, 2018, **6**(16), 6874.

16 B. Fan, D. Zhang, M. Li, W. Zhong, Z. Zeng, L. Ying, F. Huang and Y. Cao, Achieving over 16% efficiency for single-junction organic solar cells, *Sci. China: Chem.*, 2019, **62**(6), 746.

17 Y. Zou, A. Najari, P. Berrouard, S. Beaupré, B. Réda Aïch, Y. Tao and M. Leclerc, A Thieno[3,4-c]pyrrole-4,6-dione-Based Copolymer for Efficient Solar Cells, *J. Am. Chem. Soc.*, 2010, **132**(15), 5330.

18 C. Cabanetos, A. El Labban, J. A. Bartelt, J. D. Douglas, W. R. Mateker, J. M. J. Fréchet, M. D. McGehee and P. M. Beaujuge, Linear Side Chains in Benzo[1,2-*b*:4,5-*b*′] dithiophene–Thieno[3,4-c]pyrrole-4,6-dione Polymers Direct Self-Assembly and Solar Cell Performance, *J. Am. Chem. Soc.*, 2013, **135**(12), 4656.

19 J. Warnan, C. Cabanetos, A. E. Labban, M. R. Hansen, C. Tassone, M. F. Toney and P. M. Beaujuge, Ordering Effects in Benzo[1,2-*b*:4,5-*b*′]difuran-thieno[3,4-c]pyrrole-4,6-dione Polymers with >7% Solar Cell Efficiency, *Adv. Mater.*, 2014, **26**(25), 4357.

20 S. Chen, H. Yao, Z. Li, O. M. Awartani, Y. Liu, Z. Wang, G. Yang, J. Zhang, H. Ade and H. Yan, Surprising Effects upon Inserting Benzene Units into a Quaterthiophene-Based D–A Polymer–Improving Non-Fullerene Organic Solar Cells *via* Donor Polymer Design, *Adv. Energy Mater.*, 2017, **7**(12), 1602304.

21 H. Yao, R. Yu, T. J. Shin, H. Zhang, S. Zhang, B. Jang, M. A. Uddin, H. Y. Woo and J. Hou, A Wide Bandgap Polymer with Strong π–π Interaction for Efficient Fullerene-Free Polymer Solar Cells, *Adv. Energy Mater.*, 2016, **6**(15), 1600742.

22 C. L. Chochos, N. Leclerc, N. Gasparini, N. Zimmerman, E. Tatsi, A. Katsouras, D. Moschovas, E. Serpetzoglou, I. Konidakis, S. Fall, P. Lévêque, T. Heiser, M. Spanos, V. G. Gregoriou, E. Stratakis, T. Ameri, C. J. Brabec and A. Avgeropoulos, The role of chemical structure in indacenodithienothiophene-*alt*-benzothiadiazole copolymers for high performance organic solar cells with improved photo-stability through minimization of burn-in loss, *J. Mater. Chem. A*, 2017, **5**(47), 25064.

23 E. Wang, L. Hou, Z. Wang, S. Hellström, W. Mammo, F. Zhang, O. Inganäs and M. R. Andersson, Small Band Gap Polymers Synthesized *via* a Modified Nitration of 4,7-Dibromo-2,1,3-benzothiadiazole, *Org. Lett.*, 2010, **12**(20), 4470.

24 H. Zhou, L. Yang, A. C. Stuart, S. C. Price, S. Liu and W. You, Development of Fluorinated Benzothiadiazole as a Structural Unit for a Polymer Solar Cell of 7% Efficiency, *Angew.Chem., Int. Ed.*, 2011, **50**(13), 2995.

25 M. Helgesen, S. A. Gevorgyan, F. C. Krebs and R. A. J. Janssen, Substituted 2,1,3-Benzothiadiazole- And Thiophene-Based Polymers for Solar Cells – Introducing a New Thermocleavable Precursor, *Chem. Mater.*, 2009, **21**(19), 4669.

26 P. Murto, S. Tang, C. Larsen, X. Xu, A. Sandström, J. Pietarinen, B. Bagemihl, B. A. Abdulahi, W. Mammo, M. R. Andersson, E. Wang and L. Edman, Incorporation of Designed Donor–Acceptor–Donor Segments in a Host Polymer for Strong Near-Infrared Emission from a Large-Area Light-Emitting Electrochemical Cell, *ACS Appl. Energy Mater.*, 2018, **1**(4), 1753.

27 J. Zhao, Y. Li, G. Yang, K. Jiang, H. Lin, H. Ade, W. Ma and H. Yan, Efficient organic solar cells processed from hydrocarbon solvents, *Nat. Energy*, 2016, **1**, 15027.

28 H. Bin, L. Gao, Z.-G. Zhang, Y. Yang, Y. Zhang, C. Zhang, S. Chen, L. Xue, C. Yang, M. Xiao and Y. Li, 11.4% Efficiency non-fullerene polymer solar cells with trialkylsilyl substituted 2D-conjugated polymer as donor, *Nat. Commun.*, 2016, **7**, 13651.

29 Z. Genene, J. Wang, X. Meng, W. Ma, X. Xu, R. Yang, W. Mammo and E. Wang, High Bandgap (1.9 eV) Polymer with Over 8% Efficiency in Bulk Heterojunction Solar Cells, *Adv. Electron. Mater.*, 2016, **2**(7), 1600084.

30 Z. Li, X. Xu, W. Zhang, X. Meng, Z. Genene, W. Ma, W. Mammo, A. Yartsev, M. R. Andersson, R. A. J. Janssen and E. Wang, 9.0% power conversion efficiency from ternary all-polymer solar cells, *Energy Environ. Sci.*, 2017, **10**, 2212.

31 X. Li, G. Huang, N. Zheng, Y. Li, X. Kang, S. Qiao, H. Jiang, W. Chen and R. Yang, High-Efficiency Polymer Solar Cells Over 13.9% With a High VOC Beyond 1.0V by Synergistic Effect of Fluorine and Sulfur, *Sol. RRL*, 2019, **3**(4), 1900005.

32 L. Wang, D. Cai, Q. Zheng, C. Tang, S.-C. Chen and Z. Yin, Low Band Gap Polymers Incorporating a Dicarboxylic Imide-Derived Acceptor Moiety for Efficient Polymer Solar Cells, *ACS Macro Lett.*, 2013, **2**(7), 605.

33 C. B. Nielsen, R. S. Ashraf, N. D. Treat, B. C. Schroeder, J. E. Donaghey, A. J. P. White, N. Stingelin and I. McCulloch, 2,1,3-Benzothiadiazole-5,6-Dicarboxylic Imide – A Versatile Building Block for Additive- and Annealing-Free Processing of Organic Solar Cells with Efficiencies Exceeding 8%, *Adv. Mater.*, 2015, **27**(5), 948.

34 L. Lan, Z. Chen, Q. Hu, L. Ying, R. Zhu, F. Liu, T. P. Russell, F. Huang and Y. Cao, High-Performance Polymer Solar Cells Based on a Wide-Bandgap Polymer Containing Pyrrolo[3,4-f]

benzotriazole-5,7-dione with a Power Conversion Efficiency of 8.63%, *Adv. Sci.*, 2016, **3**(9), 1600032.

35 B. Fan, K. Zhang, X.-F. Jiang, L. Ying, F. Huang and Y. Cao, High-Performance Nonfullerene Polymer Solar Cells based on Imide-Functionalized Wide-Bandgap Polymers, *Adv. Mater.*, 2017, **29**(21), 1606396.

36 P. Zhu, B. Fan, X. Du, X. Tang, N. Li, F. Liu, L. Ying, Z. Li, W. Zhong, C. J. Brabec, F. Huang and Y. Cao, Improved Efficiency of Polymer Solar Cells by Modifying the Side Chain of Wide-Band Gap Conjugated Polymers Containing Pyrrolo[3,4-*f*]benzotriazole-5,7(6*H*)-dione Moiety, *ACS Appl. Mater. Interfaces*, 2018, **10**(26), 22495.

37 B. Fan, X. Du, F. Liu, W. Zhong, L. Ying, R. Xie, X. Tang, K. An, J. Xin, N. Li, W. Ma, C. J. Brabec, F. Huang and Y. Cao, Fine-tuning of the chemical structure of photoactive materials for highly efficient organic photovoltaics, *Nat. Energy*, 2018, **3**, 1051.

38 D. Dang, W. Chen, R. Yang, W. Zhu, W. Mammo and E. Wang, Fluorine substitution enhanced photovoltaic performance of a D–A1–D–A2 copolymer, *Chem. Commun.*, 2013, **49**(81), 9335.

39 K. Kawashima, T. Fukuhara, Y. Suda, Y. Suzuki, T. Koganezawa, H. Yoshida, H. Ohkita, I. Osaka and K. Takimiya, Implication of Fluorine Atom on Electronic Properties, Ordering Structures, and Photovoltaic Performance in Naphthobisthiadiazole-Based Semiconducting Polymers, *J. Am. Chem. Soc.*, 2016, **138**(32), 10265.

40 M. Zhang, X. Guo, S. Zhang and J. Hou, Synergistic Effect of Fluorination on Molecular Energy Level Modulation in Highly Efficient Photovoltaic Polymers, *Adv. Mater.*, 2014, **26**(7), 1118.

41 K. Reichenbächer, H. I. Süss and J. Hulliger, Fluorine in crystal engineering—"the little atom that could", *Chem. Soc. Rev.*, 2005, **34**(1), 22.

42 W. Huang, M. Li, L. Zhang, T. Yang, Z. Zhang, H. Zeng, X. Zhang, L. Dang and Y. Liang, Molecular Engineering on Conjugated Side Chain for Polymer Solar Cells with Improved Efficiency and Accessibility, *Chem. Mater.*, 2016, **28**(16), 5887.

43 S. Zhang, B. Yang, D. Liu, H. Zhang, W. Zhao, Q. Wang, C. He and J. Hou, Correlations among Chemical Structure, Backbone Conformation, and Morphology in Two Highly Efficient Photovoltaic Polymer Materials, *Macromolecules*, 2016, **49**(1), 120.

44 B. A. Abdulahi, X. Xu, P. Murto, O. Inganäs, W. Mammo and E. Wang, Open-Circuit Voltage Modulations on All-Polymer Solar Cells by Side Chain Engineering on 4,8-Di(thiophen-2-yl)benzo[1,2-*b*:4,5-*b*′]dithiophene-Based Donor Polymers, *ACS Appl. Energy Mater.*, 2018, **1**(6), 2918.

45 H. Benten, D. Mori, H. Ohkita and S. Ito, Recent research progress of polymer donor/polymer acceptor blend solar cells, *J. Mater. Chem. A*, 2016, **4**(15), 5340.

46 S. Kwon, H. Kang, J.-H. Lee, J. Lee, S. Hong, H. Kim and K. Lee, Effect of Processing Additives on Organic Photovoltaics: Recent Progress and Future Prospects, *Adv. Energy Mater.*, 2017, **7**(10), 1601496.

47 C. M. Proctor, M. Kuik and T.-Q. Nguyen, Charge carrier recombination in organic solar cells, *Prog. Polym. Sci.*, 2013, **38**(12), 1941.

48 Z. Li, X. Xu, G. Zhang, T. Yu, Y. Li and Q. Peng, Highly Efficient Non-Fullerene Polymer Solar Cells Enabled by Wide Bandgap Copolymers With Conjugated Selenyl Side Chains, *Sol. RRL*, 2018, **2**(10), 1800186.

49 J.-L. Wu, F.-C. Chen, Y.-S. Hsiao, F.-C. Chien, P. Chen, C.-H. Kuo, M. H. Huang and C.-S. Hsu, Surface Plasmonic Effects of Metallic Nanoparticles on the Performance of Polymer Bulk Heterojunction Solar Cells, *ACS Nano*, 2011, **5**(2), 959.

50 B. Fan, L. Ying, Z. Wang, B. He, X.-F. Jiang, F. Huang and Y. Cao, Optimisation of processing solvent and molecular weight for the production of green-solvent-processed all-polymer solar cells with a power conversion efficiency over 9%, *Energy Environ. Sci.*, 2017, **10**(5), 1243.

51 S. Li, L. Ye, W. Zhao, S. Zhang, S. Mukherjee, H. Ade and J. Hou, Energy-Level Modulation of Small-Molecule Electron Acceptors to Achieve over 12% Efficiency in Polymer Solar Cells, *Adv. Mater.*, 2016, **28**(42), 9423.

52 F. Zhao, S. Dai, Y. Wu, Q. Zhang, J. Wang, L. Jiang, Q. Ling, Z. Wei, W. Ma, W. You, C. Wang and X. Zhan, Single-Junction Binary-Blend Nonfullerene Polymer Solar Cells with 12.1% Efficiency, *Adv. Mater.*, 2017, **29**(18), 1700144.

53 A. K. K. Kyaw, D. H. Wang, D. Wynands, J. Zhang, T.-Q. Nguyen, G. C. Bazan and A. J. Heeger, Improved Light Harvesting and Improved Efficiency by Insertion of an Optical Spacer (ZnO) in Solution-Processed Small-Molecule Solar Cells, *Nano Lett.*, 2013, **13**(8), 3796.

54 Q. Fan, W. Su, X. Guo, Y. Wang, J. Chen, C. Ye, M. Zhang and Y. Li, Side-chain engineering for efficient non-fullerene polymer solar cells based on a wide-bandgap polymer donor, *J. Mater. Chem. A*, 2017, **5**(19), 9204.

55 J. K. J. vanDuren, X. Yang, J. Loos, C. W. T. Bulle-Lieuwma, A. B. Sieval, J. C. Hummelen and R. A. J. Janssen, Relating the Morphology of Poly(p-phenylene vinylene)/Methanofullerene Blends to Solar-Cell Performance, *Adv. Funct. Mater.*, 2004, **14**(5), 425.